Basic Concepts in Polymer Melt Rheology and Their Importance in Processing

Chapter · January 2012

DOI: 10.1002/9781118140611.ch1

2 authors:

John Vlachopoulos
McMaster University

Nickolas D. Polychronopoulos
The Centre for Research and Technology, Hellas

CHAPTER 1

BASIC CONCEPTS IN POLYMER MELT RHEOLOGY AND THEIR IMPORTANCE IN PROCESSING

JOHN VLACHOPOULOS[1] and NICKOLAS POLYCHRONOPOULOS[2]
[1] Department of Chemical Engineering, McMaster University, Hamilton, ON, Canada
[2] Polydynamics, Inc., Dundas, ON, Canada

CONTENTS

Applied Polymer Rheology: Polymeric Fluids with Industrial Applications, First Edition.
Edited by Marianna Kontopoulou.

1.1 INTRODUCTION

The vast majority of the nearly 250 million tons of polymers produced annually are thermoplastics, which are melted by heating, shaped by flowing through dies or filling of molds, and subsequently solidified into final useful products. The melt processing of thermoplastics is, to a large extent, determined by flow behavior, which in turn depends on structure and the processing conditions of temperature and pressure. The relations of structure, processing, and properties of polymers are of paramount importance in all their applications as film, sheet, pipe, tubing, profiles, wire and cable coatings, containers, appliance housings, automotive, and aerospace parts and as numerous other products.

Molten polymers exhibit rather unusual flow behavior and some rather counterintuitive phenomena, as it is explained in several books [1–14] and numerous publications. In fact, the majority of publications in rheology, the science of deformation and flow of matter, deal with polymer melts and solutions. First, rheological measurements are necessary for process equipment design. Knowing the viscosity as a function of shear rate permits the calculation of pressures and production rates. Process troubleshooting and process optimization can be carried out by detailed rheological characterization, as it will become apparent in the subsequent sections and chapters of this book. Some rheological measurements are sensitive indicators of polymer structure, such as molecular weight, molecular weight distribution, and chain branching. In fact, the sensitivity and frequently simplicity of some rheological characterization methods are the main reasons for the success on rheology in polymer processing. Textbooks on polymer processing [15–25] are mainly devoted to describing how rheological measurements can be combined with fluid mechanical and heat-transfer principles for the prediction of how molten polymers flow through extruders, channels, dies, molds, and other types of equipment.

1.2 VISCOSITY OF POLYMER MELTS

Viscosity represents the resistance to shearing, i.e., flow of imaginary fluid slices like the motion of a deck of cards. Referring to Figure 1.1, we can define

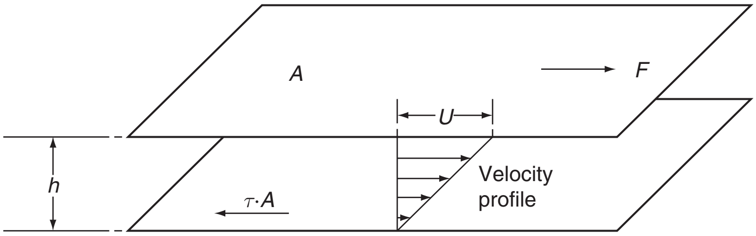

FIGURE 1.1 Simple shear flow.

viscosity as the ratio of the imposed *shear stress* (force F, applied tangentially, divided by the area A), and the shear rate (velocity U, divided by the gap h)

$$\eta = \frac{\text{Shear Stress}}{\text{Shear Rate}} = \frac{F/A}{U/h} = \frac{\tau}{\dot{\gamma}} \tag{1.1}$$

This relation is known as Newton's Law of Viscosity. When the viscosity is independent of the shear rate, a fluid is called Newtonian. Molten polymers have viscosities dependent on shear rate, exhibit several other unusual flow properties, and are referred to as non-Newtonian.

One remarkable property of polymeric liquids is their *shear-thinning* behavior (also known as pseudo-plastic behavior). As the shear rate increases, the viscosity decreases, as shown in Figure 1.2. This reduction of viscosity is due to molecular alignments and disentanglements of the long polymer chains. The higher the shear rate, the easier it is for polymers to flow through dies and process equipment.

The most frequently used model to express the shear-thinning behavior of polymers is the power law:

$$\eta = m\dot{\gamma}^{n-1} \tag{1.2}$$

This expression is a straight line when plotted on double logarithmic coordinates. The value of the consistency index m can be obtained from the intercept at $\dot{\gamma} = 1$. The exponent $n - 1$ is the slope, because

$$\log \eta = \log m + (n - 1) \log \dot{\gamma} \tag{1.3}$$

This model is not suitable for fitting low shear rate data because the viscosity predicted approaches infinity as the shear rate goes to zero, while polymeric liquids exhibit a characteristic Newtonian plateau at very low shear rates.

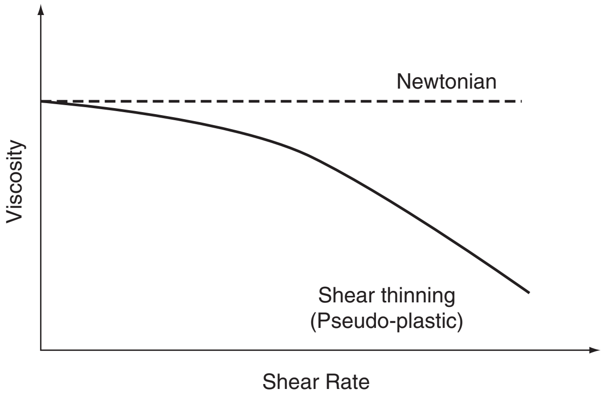

FIGURE 1.2 Newtonian and shear-thinning viscosity behavior.

For $n = 1$, the power law model reduces to Newton's law (constant viscosity). As n decreases, the polymer becomes more shear thinning. The power law exponent of commercial polymers varies between 0.8 (for some polycarbonate, PC, grades) and 0.2 (for some rubber compounds). For various polyethylene (PE) grades, the range is $0.3 < n < 0.6$, and depends on molecular weight and chain branching and does not change much with temperature. The consistency m varies a lot with temperature and under usual processing conditions the consistency index for the most common molten polymers varies between 1000 $\mathrm{Pa\cdot s}^n$ (for some polyethylene terephthalate, PET, resins) to 100,000 $\mathrm{Pa\cdot s}^n$ for highly viscous rigid polyvinyl chloride (PVC). The value depends on chain mobility and molecular weight.

During single-screw extrusion, shear rates may reach $200\,\mathrm{s}^{-1}$ in the screw channel near the barrel wall, and much higher between the flight tips and the barrel. At the die lip exit the shear rate can reach or exceed $1000\,\mathrm{s}^{-1}$. During cavity filling in injection molding shear rates can reach $10{,}000\,\mathrm{s}^{-1}$ and in some wire-coating applications shear rates may exceed $100{,}000\,\mathrm{s}^{-1}$. However, in the process of rotational molding shear rates are much less than $1\,\mathrm{s}^{-1}$.

Melt index (MI), melt flow index (MFI), or melt flow rate (MFR) (for polypropylene) refers to the grams per 10 min pushed out of a die of prescribed dimensions according to an ASTM Standard [4] under the action of a specified load, as shown in Figure 1.3. For PE (ASTM D-1238) the load is 2.16 kg and the die dimensions are $D = 2.095$ mm and $L = 8$ mm. The experiment is carried out

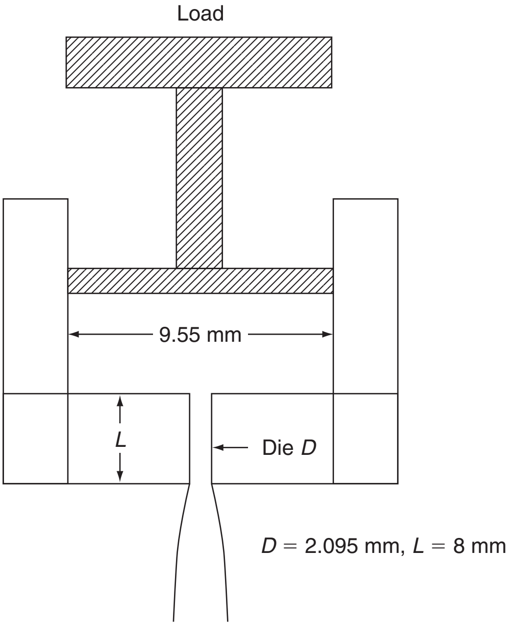

FIGURE 1.3 Schematic of a melt indexer.

at 190°C. For PP, the same load and die dimensions are used, but the experiment is carried out at 230°C.

When measuring the melt index with a 2.16-kg load, the wall shear stress can be calculated to be $\tau_w = 1.94 \times 10^4$ Pa, and the wall shear rate approximately $\dot{\gamma} = (1838/\rho) \times MI$, where ρ is the melt density in kg/m^3. Assuming $\rho = 766\,\text{kg/m}^3$ for a typical PE melt, we get $\dot{\gamma} = 2.4 \times MI$. A low melt index means a high molecular weight, highly viscous polymer. A high melt index means a low molecular weight, low viscosity polymer. When the melt index is <1, the material is said to have a fractional melt index. Such materials are used for film extrusion. For some film grades MI can be <0.1. Most extrusion PE grades seldom exceed MI = 12, however, for injection molding, MI is usually in the range of 5–50.

The MI (inversely) corresponds to just one point on a viscosity curve (usually at low shear rates). Frequently, the so-called high load melt index (HLMI) is measured, usually with either a 2.16-kg or a 10-kg load on the melt indexer. From two points it is possible to obtain a power law viscosity fit, but such approximations should always be used with extreme caution due to inherent inaccuracies in the measurement method.

For fully developed pressure driven axial flow (*z* direction) of polymeric fluid in a tube of radius *R*, the velocity profile is quasi-parabolic, the shear stress varies linearly with the radius and the shear rate nonlinearly as shown in Figure 1.4.

For Newtonian fluids, the wall shear rate is given by

$$\dot{\gamma}_w = \frac{4Q}{\pi R^3} \tag{1.4}$$

This relation is referred to as apparent shear rate when used in non-Newtonian flows. A correction is necessary (Rabinowitsch correction) for shear thinning fluids. For the power law model, the true (Rabinowitsch corrected) shear rate becomes

$$\dot{\gamma}_w = \frac{3n+1}{4n}\frac{4Q}{\pi R^3} \tag{1.5}$$

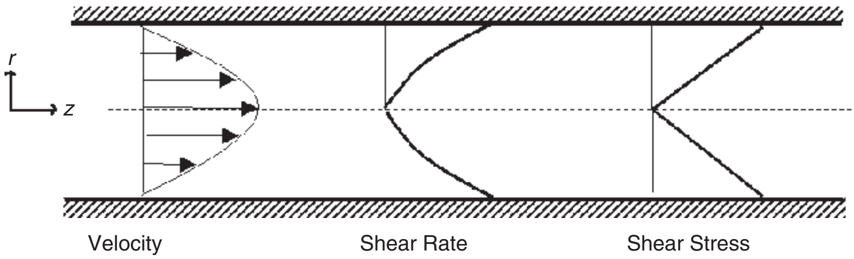

FIGURE 1.4 Velocity, shear rate, and shear stress profiles for pressure-driven flow through a tube of radius *R*.

This means that for a material with a power law exponent $n = 0.4$ (very common for several commercial polymer grades), the relation between apparent and true shear rates is given by

$$\dot{\gamma}_{\text{true}} = 1.375 \times \dot{\gamma}_{\text{apparent}} \tag{1.6}$$

The above equations are used in capillary viscometry for measurement of viscosity from pressure drop ΔP versus flow rate Q data.

The pressure drop ΔP is measured in the reservoir of the viscometer, and at the entrance to the capillary there is an excess pressure drop ΔP_e. The easiest way to determine the excess pressure drop ΔP_e is to carry out the experiment using a twin-bore viscometer having two capillaries. One of them has very short length ($L = 0$), and the pressure drop recorded is essentially the excess pressure due to the entrance (orifice). This correction is necessary when capillaries are relatively short ($L/R < 50$) and is known as the Bagley correction. The Bagley correction is usually expressed as

$$n_{\text{B}} = \frac{\Delta P_e}{2\tau_w} \tag{1.7}$$

The Bagley correction (n_{B}) may reach perhaps 20 when polymeric materials are extruded near the critical stress for sharkskin. For a Newtonian fluid the value for n_{B} is 0.587. For information on the Bagley correction and entrance and exit pressure drops the reader is referred to the monographs by Han [7].

Without the Rabinowitsch and Bagley corrections there can be significant errors in viscosity data obtained from capillary instruments.

In addition to the power law model, two other expressions are frequently used for better fitting of data over the entire range and to include the Newtonian plateau at low shear rates.

1. The Carreau–Yasuda model:

$$\eta = \eta_{\text{o}}\left(1 + (\lambda\dot{\gamma})^{a}\right)^{\frac{n-1}{a}} \tag{1.8}$$

   where η_{o} is the viscosity at zero shear and λ, a, and n are fitted parameters.
2. The Cross model:

$$\eta = \frac{\eta_{\text{o}}}{1 + (\lambda\dot{\gamma})^{1-n}} \tag{1.9}$$

   where η_{o} is the zero shear viscosity and λ and n are fitted parameters. Note that in this model when $\lambda = 1/\dot{\gamma}, \eta = \eta_{\text{o}}/2$

Capillary viscometers are usually used for the shear rate range from $1\,\text{s}^{-1}$ to $3000\,\text{s}^{-1}$. The lower limit is determined by the ability of pressure gauges to measure low pressures, with accuracy, and the high limit is determined by instabilities, wall slip, and viscous heating phenomena. Rotational viscometers are usually used for the range 10^{-2} to $5\,\mathrm{s}^{-1}$. At higher rotational speeds, secondary flows and instabilities may occur that invalidate the simple shear assumption. For more information about viscosity measurements, the reader is referred to Macosko [2].

The viscosity of polymer melts varies with temperature and for most polyolefins it obeys the Arrhenius relation is the form

$$\eta = \eta_{ref} \exp\left[\frac{E}{R}\left(\frac{1}{T} - \frac{1}{T_{ref}}\right)\right] \tag{1.10}$$

where E is the activation energy, R the gas constant and T_{ref} is the reference temperature.

In polymer processing this relation is frequently simplified into a simple exponential, which applies over a shorter temperature range but it is good enough for most extrusion calculations and simulations

$$\eta = \eta_{ref} \cdot \exp(-b \cdot \Delta T) \tag{1.11}$$

The temperature sensitivity coefficient b is usually between 0.01 and $0.1\,{}^{\circ}\mathrm{C}^{-1}$. For a linear polymer, high density polyethylene (HDPE) the value of b is roughly 0.01, while for a branched low density polyethylene (LDPE) it may reach 0.03.

The viscosity increases with pressure in the form

$$\eta(p) = \eta(0) \cdot \exp(\alpha \cdot p) \tag{1.12}$$

The coefficient is probably of the order $2 \times 10^{-8}\,\mathrm{Pa}^{-1}$. This means for a pressure increase of 10 MPa the viscosity will go up by 22%. Cogswell [3] expresses pressure dependence in terms of an equivalent temperature change. His results suggest that applying 10 MPa is equivalent to decreasing the temperature by about 5 °C. Usually, pressure dependence of viscosity is not taken into consideration in extrusion, but it is necessary in injection molding calculations and simulations. Pressure drops in die extrusion may reach at most 50 MPa, while in injection molding cavity filling the pressure may reach 200 MPa.

The effects of factors such as shear rate, molecular weight distribution, pressure, filler, temperature and additives on viscosity are summarized in Figure 1.5, following Cogswell [3]. Linear narrow molecular weight distribution polymers, such as metallocene catalyzed polyethylenes, are more viscous than their broad distribution counterparts. Fillers may increase viscosity (greatly). Pressure increases viscosity (negligible under usual extrusion conditions, but important in injection molding). Various additives, such as processing aids and lubricants, are available and are designed to decrease viscosity. The zero shear viscosity increases dramatically with the weight average molecular weight:

$$\eta_o = \mathrm{const}\, M_w^{3.4} \tag{1.13}$$

For some metallocene catalyzed PEs with long chain branching, the exponent might be much higher (perhaps 6.0).

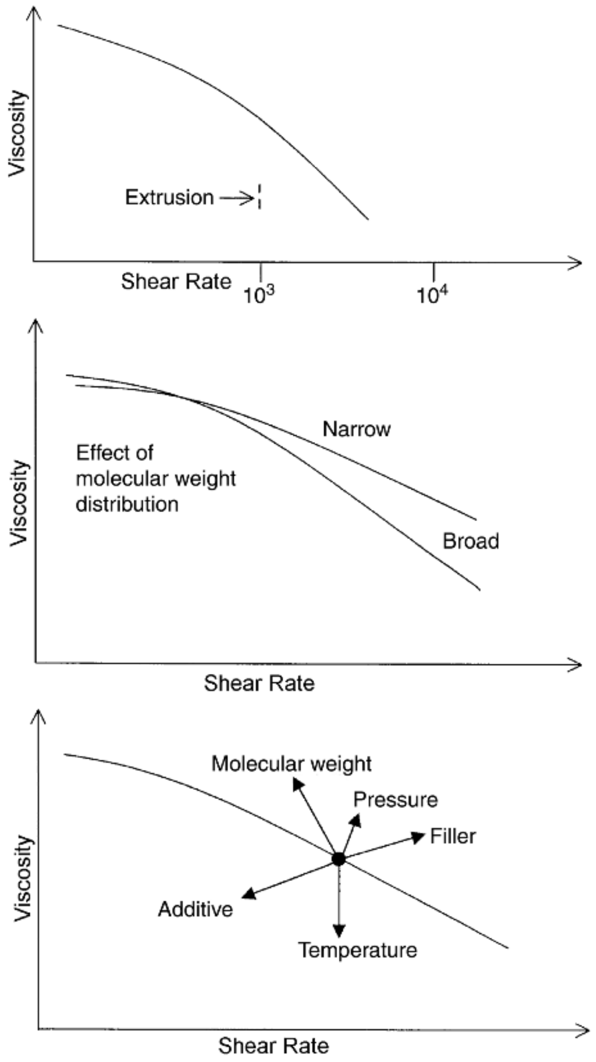

FIGURE 1.5 The influence of various parameters on polymer viscosity.

In the above discussion of viscosity measurements, the assumption is made that the no-slip condition on the die wall is valid. This is, however, not always the case. In fact, at shear stress levels of about 0.1 MPa for PE, slip occurs. Wall slip is related to the sharkskin phenomenon [26, 27]. Wall slip is measured by the Mooney method in which the apparent shear rate ($4Q/\pi R^3$) is plotted against $1/R$ for several capillaries having different radii. In the absence of slip, the plot is horizontal. The slope of the line is equal to 4 × (slip velocity), as explained by Dealy and Wissbrun [5].

1.3 EXTENSIONAL VISCOSITY AND MELT STRENGTH

Extensional (or elongational) viscosity is the resistance of a fluid to extension [1, 2]. While stretching a low-viscosity fluid like water is difficult to imagine, polymer melts exhibit measurable resistance. In fact, about 100 years ago, Trouton measured the stretching and shearing resistance of stiff liquids, including pitch, and found that the extensional to shear viscosity ratio is equal to 3.

$$\frac{\eta_e}{\eta} = 3 \tag{1.14}$$

This relation, known as the Trouton ratio, is valid for all Newtonian fluids and has a rigorous theoretical basis that confirms Trouton's experiments.

Measuring elongational viscosity is considerably more difficult than measuring shear viscosity. One device used involves capillary extrusion and subsequent stretching with a pair of rollers. The maximum force required to break the extruded strand is referred to as *melt strength*. In practice, the terms *extensional viscosity* and *melt strength* are sometimes confused. Figure 1.6. shows extensional viscosity as a function of stretch rate ($\dot{\varepsilon}$), and compares it to the shear viscosity as a function of shear rate ($\dot{\gamma}$). Melt strength is an engineering measure of resistance to extension. Several extrusion processes involve extension, such as film blowing, melt spinning, thermoforming, and blow molding.

The excess pressure drop encountered in flow from a large reservoir to a smaller diameter capillary is due to elongational viscosity. In fact, Cogswell [3]

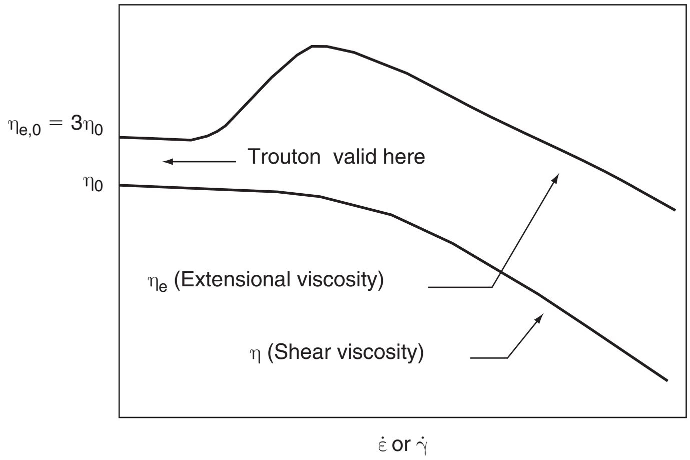

FIGURE 1.6 Extensional and shear viscosity as a function of stretch and shear rate, respectively.

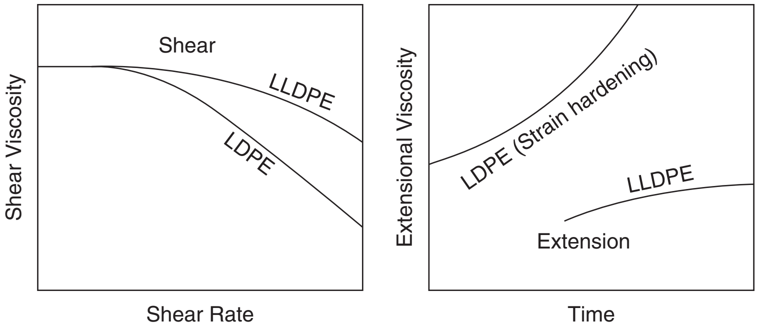

FIGURE 1.7 Schematic representation of LDPE and LLDPE behavior in shear and extension.

has developed a method for measurement of elongational viscosity η_e from excess pressure drop ΔP_e (i.e., the Bagley correction):

$$\eta_e = \frac{9(n+1)^2(\Delta P_e)^2}{32\eta\dot{\gamma}^2} \tag{1.15}$$

$$\dot{\varepsilon} = \frac{4\eta\dot{\gamma}^2}{3(n+1)\Delta P_e} \tag{1.16}$$

Shear and extensional viscosity measurements reveal that LLDPE (which is linear) is "stiffer" than LDPE (branched) in shear, but "softer" in extension. In extension, the linear LLDPE chains slide by without getting entangled. However, the long branches of the LDPE chains result in significantly larger resistance in extension. In the film-blowing process, LDPE bubbles exhibit more stability because of their high extensional viscosity. Typical LDPE and LLDPE behavior in shear and extension is shown in Figure 1.7. LDPE is often blended with LLDPE to improve the melt strength and consequently bubble stability in film blowing. Most polypropylene (PP) grades are known to exhibit very low melt strength. However, recent advances in polymer chemistry have led to the production of some high melt strength PP grades (with long chain branching).

Measurements of elongational viscosity have been plagued by experimental complexities, lack of repeatability, and considerable inaccuracies. The recently developed SER rheometer [12, 28] seems to have put these problems at rest and it is expected to play a significant role in the analysis and optimization of polymer processes in the near future.

1.4 NORMAL STRESS DIFFERENCES AND EXTRUDATE SWELL

Stress is defined as force divided by the area on which it acts. It has units of N/m^2 (Pascal, Pa) in SI. When a force is acting tangentially on a surface, the corresponding stress is referred to as *shear stress*. When a force is perpendicular (normal) to a surface, it is termed *normal stress*. Pressure is a normal stress. When a fluid flows through a conduit, it is acted by the normal (pressure) forces, and it exerts both normal and shear (stress) forces on the conduit walls. For flow through a planar die the shear stress is zero at the mid-plane and maximum at the wall, while the corresponding velocity profile is quasi-parabolic.

Weissenberg discovered in the 1940 s [1, 2] that polymer solutions and melts, when subjected to shearing, tend to develop normal stresses that are unequal in the x (direction of flow), y, and z (normal directions) planes, which are added to or subtracted from the local pressure. They are generated because a polymer's long molecular chains exhibit anisotropic or nonuniform properties when they flow. Any further explanation of the physical origin of normal stresses is likely to be controversial. When an (elastic) polymer solution or melt flows along a pressure gradient, it is less compressed in the direction of flow than in the other two normal directions.

The first normal stress difference N_1 is defined as the total normal stress in the direction of the flow (τ_{xx}) minus the perpendicular (τ_{yy}) stress.

$$N_1 = \sigma_{xx} - \sigma_{yy} = (-P + \tau_{xx}) - (-P + \tau_{yy}) = \tau_{xx} - \tau_{yy} \tag{1.17}$$

The second normal stress difference is

$$N_2 = \sigma_{yy} - \sigma_{zz} = (-P + \tau_{yy}) - (-P + \tau_{zz}) = \tau_{yy} - \tau_{zz} \tag{1.18}$$

We use normal stress differences rather than just normal stresses to remove the value of the pressure present. Experiments show that N_1 is positive for usual polymers (i.e., extensive, while the compressive pressure forces are negative). N_2 is negative and of the order of 20% of N_1 for most common polymers. N_1 is very sensitive to the high molecular weight tail of a polymer. Broad molecular weight distribution polymers exhibit high N_1 values.

The normal stress differences can be very large in high shear-rate extrusion through the lips of a die. Some authors suggest a variation for the normal stress difference at the wall in the form

$$N_{1w} = A\tau_w^b \tag{1.19}$$

The stress ratio

$$S_R = \frac{N_{1w}}{2\tau_w} \tag{1.20}$$

can reach a value of 10 or more at the onset of melt fracture.

The rod-climbing effect observed by Weissenberg when a cylinder rotates in a polymeric liquid is due to some sort of "strangulation" force exerted by the extended polymer chains (Fig. 1.8a), which results in an upward movement

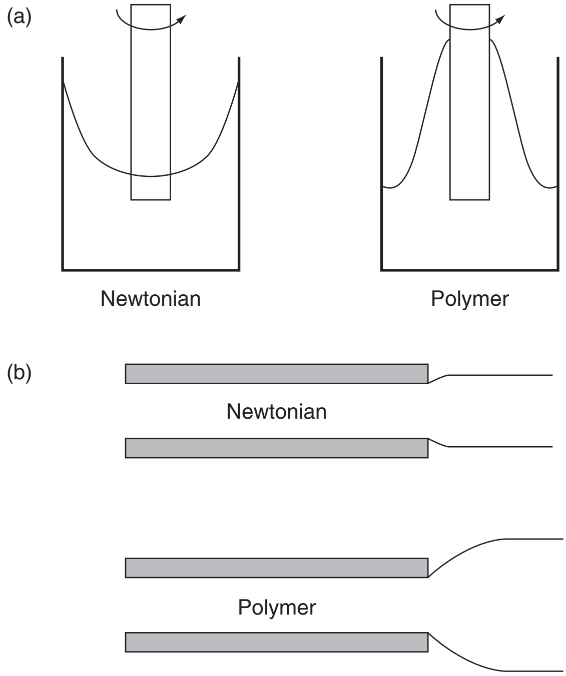

FIGURE 1.8 (a) Rod climbing (Weissenberg) effect in polymeric fluids, (b) Extrudate swell.

normal to the direction of rotation (normal stress difference). The extrudate swell phenomenon [1, 29] (Fig. 1.8b) is due mainly to the contraction of the exiting polymer that is under extension in the die due to N_1. The uneven extension/compression in the various directions results in a number of unusual flow patterns and instabilities. The secondary flow patterns in square channels observed by Dooley and co-workers [30, 31] are due to the second normal stress difference. Bird et al. [1] state: "A fluid that's macromolecular is really quite weird, in particular the big normal stresses the fluid possesses give rise to effects quite spectacular."

In extrusion through dies the extrudate diameter (*d*) is larger than the die diameter (*D*). Extrudate swell ratios (d/D) reach values of 400% or more, under certain conditions. This phenomenon (also known as die swell) has been studied by several researchers. While the primary mechanism is release of normal stresses at the exit, other effects are also important. Extrudate swell is largest for zero length dies (i.e., orifices). It decreases for the same throughput with increasing die length due to fading memory as the residence time in the die increases. Even Newtonian fluids exhibit some swell exiting dies (13% for round extrudates, 19% for planar extrudates). This Newtonian swell is due to streamline rearrangement at the exit. The swell ratio can be influenced by thermal effects due to viscosity differences between the walls and die center. Maximum thermal swell can be obtained when a hot polymer flows through a die with colder walls. Swell ratio of about 5% on top of other mechanisms can be obtained from temperature differences. For linear polymers the swell ratio increases as the molecular weight distribution broadens.

Several attempts have been made to predict extrudate swell through equations relating the swell ratio d/D (extrudate diameter/die diameter) to the first normal stress difference at the wall N_{1w}. Based on the theory of rubber elasticity, the following equation is obtained [29]

$$N_{1w} = 2\tau_w \left(3 \left[\left(\frac{d}{D} \right)^4 + 2 \left(\frac{d}{D} \right)^{-2} - 3 \right] \right)^{\frac{1}{2}} \tag{1.21}$$

Based on stress release for a Maxwell fluid (described later in the chapter) exiting from a die, Tanner's equation can be derived [6, 29]

$$N_{1w} = 2\sqrt{2}\,\tau_w \left[\left(\frac{d}{D} - 0.13 \right)^6 - 1 \right]^{\frac{1}{2}} \tag{1.22}$$

Although this equation has a more rigorous derivation and theoretical basis, the rubber elasticity theory is believed to give better predictions. Unambiguous evaluations are virtually impossible to carry out because there are no reliable methods for measuring N_{1w} at high shear rates and stresses. At low shear rates (up to perhaps $1\,\mathrm{s}^{-1}$) the first normal stress difference can be determined by measuring the separation force that develops in a cone-and-plate instrument due to the Weissenberg effect.

1.5 STRESS RELAXATION AND DYNAMIC MEASUREMENTS

When flow stops, the stresses become immediately zero for small molecule Newtonian fluids like water or glycerin. For polymer melts, the stresses decay exponentially after flow stops. Stress relaxation can be measured in a parallel plate or a cone-and-plate rheometer by applying a given shear rate level (rotation speed/gap) and measuring the stress decay after the rotation is brought to an abrupt stop. Such tests, however, are not performed routinely, because of experimental limitations associated with abrupt stopping of strain and stress measurement decay over more than three orders of magnitude with one transducer.

Dynamic measurements involve the response of a material to an imposed sinusoidal stress or strain on a parallel plate or cone-and-plate instrument. A perfectly elastic material that behaves like a steel spring, by imposition of extension (strain), would develop stresses that would be in-phase with the strain, because

$$\text{Stress}(\tau) = \text{Modulus(G)} \times \text{Strain}(\gamma) \tag{1.23}$$

However, for a Newtonian fluid subjected to a sinusoidal strain, the stress and strain will not be in phase because of the time derivative (strain rate) involved

$$\tau = \eta\dot{\gamma} \tag{1.24}$$

$$\begin{aligned} \tau = \eta\frac{d\gamma}{dt} = \eta\frac{d}{dt}(\gamma_o \sin \omega t) = \eta\omega\gamma_o \cos \omega t \\ = \eta\omega\gamma_o \sin(\omega t + 90^\circ) \end{aligned} \tag{1.25}$$

where ω is frequency of oscillation. That is, a Newtonian fluid would exhibit 90° phase difference between stress and strain. Polymeric liquids that are partly viscous and partly elastic (viscoelastic) will be $0 \leq \varphi \leq 90^\circ$ out of phase.

We can define

$$\begin{aligned} G'(\omega) &= \frac{\text{in-phase stress}}{\text{maximum strain}} \quad \begin{matrix}\text{storage}\\ \text{modulus}\\ \text{(elastic part)}\end{matrix} \\ G''(\omega) &= \frac{\text{out-of-phase stress}}{\text{maximum strain}} \quad \begin{matrix}\text{loss}\\ \text{modulus}\\ \text{(viscous part)}\end{matrix} \end{aligned} \tag{1.26}$$

where ω ranges usually from 0.01 to 500 rad/s. Larger G' implies more elasticity. Further, we can define the dynamic viscosity

$$\begin{aligned} \eta' &= \frac{G''}{\omega} \\ \eta'' &= \frac{G'}{\omega} \end{aligned} \tag{1.27}$$

and the magnitude of the complex viscosity

$$|\eta^*| = (\eta'^2 + \eta''^2)^{1/2} \tag{1.28}$$

An empirical relationship called the Cox-Merz rule states that the shear rate dependence of the steady state viscosity η is equal to the frequency dependence of the complex viscosity η^*, that is

$$\eta(\dot{\gamma}) = |\eta^*(\omega)| \tag{1.29}$$

The usefulness of this rule, which holds for most conventional polymers, is that while steady measurements of shear viscosity are virtually impossible for shear

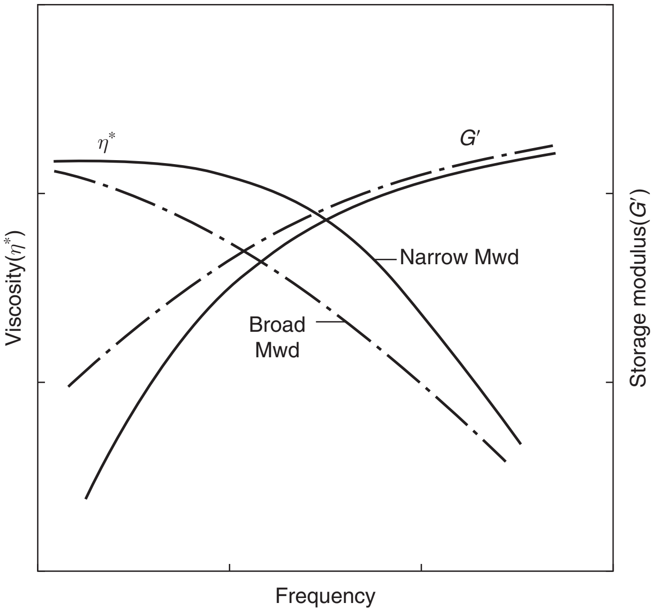

FIGURE 1.9 Storage modulus G' and dynamic viscosity η^* behavior of broad and narrow molecular weight distribution polymers.

rates larger than 5/s with rotational instruments, the dynamic measurements can easily be carried out up to 500 rad/s (corresponds to shear rate of 500 s^{-1}) or even higher. Thus the full range of viscosity needed in extrusion can be covered.

Some typical results involving narrow and broad molecular weight distribution samples are shown in Figure 1.9. The relative behavior of G' versus ω can be used to identify whether a sample is of narrow or broad molecular weight distribution [5]. In fact, from the crossover point where $G' = G''$, it is possible to get a surprisingly good estimate of the polydispersity M_w/M_n for PP [32]. For such experiments to be meaningful the imposed strain amplitude must be low, so that the measured G' and G'' values do not vary with the strain, but they are intrinsic properties of the polymer structure. This is the region of the so-called linear viscoelasticity.

Another interesting result is the relation between storage modulus and first normal stress difference at very small deformations ($\omega \to 0$, $\gamma \to 0$)

$$2G' = N_1 \tag{1.30}$$

For higher frequencies an expression developed by Laun [33, 5] is used:

$$N_1 = 2\frac{G'}{\omega^2}\left[1 + \left(\frac{G'}{G''}\right)^2\right]^{0.7} \tag{1.31}$$

It is possible to measure N_1 using a cone-and-plate rotational rheometer. The Weissenberg effect results in a separating force between the cone and the plate which can be measured to give N_1.

Instruments capable of measuring N_1 require high precision construction and very sensitive force gauges. However, measurement of G', the storage modulus, can be carried out more easily.

1.6 CONSTITUTIVE EQUATIONS

Constitutive equations are relations between stresses and strains (deformations). In its simplest form, the Newtonian equation is a linear relation between the shear stress and the shear rate

$$\tau = \eta\dot{\gamma} = \eta\frac{dv_x}{dy} \tag{1.32}$$

This is valid for simple shear flow between two flat plates, as explained earlier in this chapter, and it is directly applicable to unidirectional flows. In polymer processing, however, most interesting flow problems require two- or three-dimensional analyses, of creeping (low Reynolds number, $\mathrm{Re} << 1$) flows. For incompressible steady flow the mass conservation equation is

$$\nabla \cdot \overline{v} = 0 \tag{1.33}$$

or

$$\frac{\partial v_x}{\partial x} + \frac{\partial v_y}{\partial y} + \frac{\partial v_z}{\partial z} = 0 \tag{1.34}$$

and the momentum equation

$$0 = -\nabla P + \nabla \cdot \overline{\overline{\tau}} \tag{1.35}$$

where P is the pressure (which is a scalar) and $\overline{\overline{\tau}}$ the stress, which is a (second order) tensor

$$\overline{\overline{\tau}} \Rightarrow \begin{pmatrix} \tau_{xx} & \tau_{xy} & \tau_{xz} \\ \tau_{yx} & \tau_{yy} & \tau_{yz} \\ \tau_{zx} & \tau_{zy} & \tau_{zz} \end{pmatrix} \tag{1.36}$$

To generalize the Newtonian equation in three dimensions we must propose a linear relation between stress components and strain rate components. The strain rate tensor is

$$\overline{\overline{D}} = \frac{1}{2}(\nabla\overline{v} + \nabla\overline{v}^T) = \frac{1}{2}\left(\frac{\partial v_i}{\partial x_j} + \frac{\partial v_j}{\partial x_i}\right) \tag{1.37}$$

$$\overline{\overline{D}} \Rightarrow \begin{pmatrix} D_{xx} & D_{xy} & D_{xz} \\ D_{yx} & D_{yy} & D_{yz} \\ D_{zx} & D_{zy} & D_{zz} \end{pmatrix} \tag{1.38}$$

where $D_{xx} = \frac{1}{2}\left(\frac{\partial \upsilon_x}{\partial x} + \frac{\partial \upsilon_x}{\partial x}\right) = \frac{\partial \upsilon_x}{\partial x}$, $D_{xy} = \frac{1}{2}\left(\frac{\partial \upsilon_x}{\partial y} + \frac{\partial \upsilon_y}{\partial x}\right)$, and similarly the other components can be written out explicitly in terms of the components in the x, y, and z directions.

The Newtonian constitutive equation is generalized in the form

$$\overline{\overline{\tau}} = \eta(2\,\overline{\overline{D}}) \tag{1.39}$$

This means that $\tau_{xx} = \eta(2D_{xx}) = 2\eta\frac{\partial \upsilon_x}{\partial x}$, $\tau_{xy} = \eta(2D_{xy}) = \eta\left(\frac{\partial \upsilon_x}{\partial y} + \frac{\partial \upsilon_y}{\partial x}\right)$ etc.

The models expressing shear thinning behavior of polymer melts (power – law, Carreau–Yasuda and Cross) are generalized by replacing $\dot{\gamma}$ by the function (II_D) which is the second invariant of the strain rate tensor $2\,\overline{\overline{D}}$. It is called *invariant*, because this quantity remains unchanged under rotation of the coordinate axes. It is given in rectangular, cylindrical, and spherical coordinates in Table 1.1. Thus we have the generalized power law equation written as

$$\eta = m(II_D)^{\frac{n-1}{2}} \tag{1.40}$$

TABLE 1.1 The Second Invariant Strain Rate Tensor in Rectangular, Cylindrical, and Spherical Coordinates.

Rectangular

$$II_D = 2\left[\left(\frac{\partial \upsilon_x}{\partial x}\right)^2 + \left(\frac{\partial \upsilon_y}{\partial y}\right)^2 + \left(\frac{\partial \upsilon_z}{\partial z}\right)^2\right] + \left[\frac{\partial \upsilon_y}{\partial x} + \frac{\partial \upsilon_x}{\partial y}\right]^2 + \left[\frac{\partial \upsilon_z}{\partial y} + \frac{\partial \upsilon_y}{\partial z}\right]^2 + \left[\frac{\partial \upsilon_x}{\partial z} + \frac{\partial \upsilon_z}{\partial x}\right]^2$$

Cylindrical

$$II_D = 2\left[\left(\frac{\partial \upsilon_r}{\partial r}\right)^2 + \left(\frac{1}{r}\frac{\partial \upsilon_\theta}{\partial \theta} + \frac{\upsilon_r}{r}\right)^2 + \left(\frac{\partial \upsilon_z}{\partial z}\right)^2\right] + \left[r\frac{\partial}{\partial r}\left(\frac{\upsilon_\theta}{r}\right) + \frac{1}{r}\frac{\partial \upsilon_r}{\partial \theta}\right]^2 + \left[\frac{1}{r}\frac{\partial \upsilon_z}{\partial \theta} + \frac{\partial \upsilon_\theta}{\partial z}\right]^2 + \left[\frac{\partial \upsilon_r}{\partial z} + \frac{\partial \upsilon_z}{\partial r}\right]^2$$

Spherical

$$\begin{aligned} II_D = {} & 2\left[\left(\frac{\partial \upsilon_r}{\partial r}\right)^2 + \left(\frac{1}{r}\frac{\partial \upsilon_\theta}{\partial \theta} + \frac{\upsilon_r}{r}\right)^2 + \left(\frac{1}{r\sin\theta}\frac{\partial \upsilon_\phi}{\partial \phi} + \frac{\upsilon_r}{r} + \frac{\upsilon_\theta \cot\theta}{r}\right)^2\right] \\ & + \left[r\frac{\partial}{\partial r}\left(\frac{\upsilon_\theta}{r}\right) + \frac{1}{r}\frac{\partial \upsilon_r}{\partial \theta}\right]^2 + \left[\frac{\sin\theta}{r}\frac{\partial}{\partial \theta}\left(\frac{\upsilon_\phi}{\sin\theta}\right) + \frac{1}{r\sin\theta}\frac{\partial \upsilon_\theta}{\partial \phi}\right]^2 \\ & + \left[\frac{1}{r\sin\theta}\frac{\partial \upsilon_r}{\partial \phi} + r\frac{\partial}{\partial r}\left(\frac{\upsilon_\phi}{r}\right)\right]^2 \end{aligned}$$

Using the expression of the second invariant in rectangular coordinates, it can easily be shown that for simple shear flow (x-velocity only, varying in y-direction only) we have

$$\eta = m\left(\frac{\partial \upsilon_x}{\partial x}\right)^n \tag{1.41}$$

The above fluid model, which expresses simply the shear thinning behavior, is referred to as the generalized Newtonian fluid (GNF) in the rheological literature. This model cannot explain any of the viscoelastic flow phenomena, such as stress relaxation, normal stresses, or extrudate swell.

The simplest way to develop viscoelastic constitutive equations is to combine a model for an elastic solid

$$\tau = G\gamma_{\text{solid}} \tag{1.42}$$

where γ_{solid} is the strain, with that for a Newtonian fluid

$$\tau = \eta\dot{\gamma}_{\text{fluid}} \tag{1.43}$$

By differentiating the elastic solid equation and adding the two strain rates, we get

$$\frac{\dot{\tau}}{G} + \frac{\tau}{\eta} = \dot{\gamma} \tag{1.44}$$

or

$$\tau + \lambda\dot{\tau} = \eta\dot{\gamma} \tag{1.45}$$

where $\lambda = \eta/G$ has dimensions of time (relaxation constant).

This is known as the Maxwell model and shows that the viscoelastic nature of polymers can be described by viscosity and a relaxation time. This model can be generalized in two dimensions as follows

$$\tau_{xx} + \lambda\left[\frac{\partial \tau_{xx}}{\partial t} + \upsilon_x\frac{\partial \tau_{xx}}{\partial x} + \upsilon_y\frac{\partial \tau_{xx}}{\partial y} - 2\frac{\partial \upsilon_x}{\partial x}\tau_{xx} - 2\frac{\partial \upsilon_x}{\partial y}\tau_{yx}\right] = 2\eta\frac{\partial \upsilon_x}{\partial x} \tag{1.46}$$

$$\tau_{yy} + \lambda\left[\frac{\partial \tau_{yy}}{\partial t} + \upsilon_x\frac{\partial \tau_{yy}}{\partial x} + \upsilon_y\frac{\partial \tau_{yy}}{\partial y} - 2\frac{\partial \upsilon_y}{\partial x}\tau_{xy} - 2\frac{\partial \upsilon_y}{\partial y}\tau_{yy}\right] = 2\eta\frac{\partial \upsilon_y}{\partial y} \tag{1.47}$$

$$\tau_{xy} + \lambda\left[\frac{\partial \tau_{xy}}{\partial t} + \upsilon_x\frac{\partial \tau_{xy}}{\partial x} + \upsilon_y\frac{\partial \tau_{xy}}{\partial y} - \frac{\partial \upsilon_x}{\partial y}\tau_{yy} - \frac{\partial \upsilon_y}{\partial x}\tau_{xx}\right] = \eta\left[\frac{\partial \upsilon_x}{\partial y} + \frac{\partial \upsilon_y}{\partial x}\right] \tag{1.48}$$

$$\tau_{xy} = \tau_{yx}(\text{the stress tensor is symmetric}) \tag{1.49}$$

Actually, the above is one of the possible generalizations that satisfy mathematical invariance. In general, the Maxwell model is written as

$$\bar{\bar{\tau}} + \lambda\frac{\Delta\bar{\bar{\tau}}}{\Delta t} = 2\eta\bar{\bar{D}} \tag{1.50}$$

where the derivative $\Delta/\Delta t$ is referred to as the upper convective derivative as given in the above equations in two dimensions. There is also the lower convective derivative as well as other forms (e.g., co-rotational) which are the subject of specialized handbooks [1, 6, 7, 12] and numerous articles.

There are several possible extensions and generalizations of simple models. For example the convected Maxwell model can be written in the form

$$\bar{\bar{\tau}} + \lambda(II_D)\frac{\Delta \bar{\bar{\tau}}}{\Delta t} = 2\eta(II_D)\,\bar{\bar{D}} \tag{1.51}$$

where $\lambda(II_D)$ and $\eta(II_D)$ represent the relaxation time and the viscosity, respectively; both of them are functions of the second invariant of the strain rate tensor. In this form, the model is known as White–Metzner. When a generalization is proposed the key criterion is to satisfy the principle of material indifference, which states that the predicted response of a material must be the same for all observers irrespective of their coordinate system of reference. As a consequence of this, in the development of constitutive equations, a coordinate system that moves, rotates, and deforms with the material should be used. This requirement results in mathematically complex constitutive equations. Despite their complexity and the requirement of fitting of numerous parameters most viscoelastic constitutive equations fail to predict most of the unusual rheological phenomena exhibited by polymeric liquids. The most successful constitutive equation is the so-called *K-BKZ* integral model inspired by the theory of rubber elasticity [7] and involves more than two dozen experimentally fitted parameters (e.g., Ref. 34). Current trends involve the development of models based on macromolecular motions. De Gennes proposed the snake-like motion of polymer chains called reptation [2, 12] and deduced from scaling relations that the zero shear viscosity must be $\eta_o \approx M^{3.0}$, while experiments give $\eta_o \approx M^{3.4}$ (M is the molecular weight). Based on the reptation concept Doi and Edwards [2, 12] developed a constitutive equation that leaves much to be desired before it can be used for predicting viscoelastic flow phenomena. Several attempts were made to fix the Doi–Edwards theory [12]. The most talked about viscoelastic model recently, is the pom-pom polymer model, developed by McLeish and Larson [12, 35]. The motivation for its development was that the *K-BKZ* equation fails to predict the observed degree of strain hardening in planar extension when certain functions are adjusted to fit the observed degree of strain softening in shear. The failure to describe the rheology of long-branched polymers suggests that some new molecular insight is needed into the nonlinear relaxation processes that occur in such melts under flow. The pom-pom model uses an H-polymer structure, in which molecules contain just two branch points of chosen functionality and a backbone that links the two pom-poms. The pom-pom model exhibits rheological behavior remarkably similar to that of branched commercial melts like LDPE. It shows strain hardening in extension and strain softening in shear. It can describe both planar and uniaxial extension. The constitutive equation is an integro differential. For successful application at least 32 parameters must be obtained by fitting experimental rheological data. Of course, fitting 32 or more parameters in a complicated constitutive equation is a mathematical challenge.

Modeling polymer viscoelastic behavior has always been a controversial subject. While viscoelastic constitutive equations have contributed toward understanding of various deformation mechanisms and flow, they unfortunately have *not* provided us with quantitative predicting power for polymer process and equipment design. Very often the predictions depend on the model used for the computations and are not corroborated with experimental observations. Some viscoelastic problems can be solved with the appropriate constitutive equations, but this is still an area of academic research with very limited practical applications at the moment.

For design of polymer process equipment such as extruders, dies, and molds, computer simulations are carried out in two or three dimensions, using the GNF model. The Carreau–Yasuda and Cross models have a clear advantage over the power law because they can capture the viscosity behavior from the Newtonian plateau at low shear rates to high shear regions with substantial shear thinning.

1.7 PROBLEM SOLVING WITH THE HELP OF RHEOLOGY

1.7.1 Using the Melt Flow Index (MFI)

The MFI, a simple flow test, is used for quality control purposes and, as explained earlier in this chapter, gives a rough estimate of viscosity and indirectly the approximate average molecular weight. Despite the misgivings expressed by academic rheologists, more than 100 million tons of HDPE, LDPE, LLDPE, PP, PS, and other thermoplastics are sold annually, on the basis of solid density and the MFI, under standard conditions (2.16 kg load and 190° for polyethylene). The conversion of polymer pellets into film, sheet, pipe, profiles, automotive parts, containers, appliance housings, and numerous other products is carried out mainly in small and medium enterprises, which number over 100,000 around the world. Such companies do not possess the instruments or the know-how to carry out accurate rheological measurements and to fully get the benefit of such characterization. Frequently, original equipment manufacturers are asked to design and build processing equipment (extruders, dies and molds) without any rheological information other than the MFI. Consequently some short of zero-shear viscosity or consistency index in the power law model has to be estimated, and a power law exponent has to be chosen for any calculations or simulations. Processors extrude, injection mold, or otherwise process huge quantities of plastics without any additional controls on the incoming raw materials (pellets or powders).

Measurement of a high load melt index (usually with 21.6 or 10 kg) can provide an approximate second point on a viscosity curve, and the power law model parameters can be easily obtained [15], but they will not be very accurate due to experimental limitations of the melt indexer. The ratio HLMFI:MFI gives an indication of the degree of shear thinning, and it can be used to differentiate between two grades of the same polymer type or to assess processability. For example, the higher the HLMFI:MFI ratio the more the shear thinning and the lower the pressures and viscous heat generated.

The MFI is used for selecting a polymer grade for a particular application, depending on whether a larger or a smaller average molecular weight is more suitable. This in turn can be related to end use properties such as part failure. For example, polymers with higher molecular weight are known to have better environmental stress cracking resistance (ESCR). Consequently, polymers with lower MFI should be processed for parts required to have better ESCR. Similarly, polymers with lower MFI will produce stronger films for packaging and stronger fibers for ropes than their higher MFI counterparts.

Generally, the MFI test (preferably with two loads) can be used to give an indication on the average molecular weight, the viscosity and shear thinning, and the end-use properties, before more sophisticated and more expensive characterizations commence.

1.7.2 Using Viscosity Data

Accurate measurements of viscosity are absolutely necessary for computer simulations and rational equipment design. The data can easily be fitted to the Carreau–Yasuda or Cross viscosity models and subsequently be used in numerical analysis of molten polymer flows through channels and process equipment, by solving the appropriate differential equations for conservation of mass, momentum and energy. The Carreau–Yasuda and Cross viscosity curves are smooth from very low to very high shear rates, and the various numerical analysis schemes (finite differences, finite elements, boundary elements) do not offer any special problems associated with the viscosity functions. The power law model, which permits closed-form solutions for some unidirectional and lubrication approximation flow problems, may give some numerical difficulties (stability, convergence) due to the fact that the viscosity tends to infinity as the shear rate approaches zero. Obviously, there is no advantage in choosing the simple power law model whenever finite differences or finite elements are involved.

The viscosity curve itself can be used for polymer grade identification purposes. The zero-shear viscosity is related to the average molecular weight as discussed earlier in this chapter. To obtain an accurate value of the zero-shear viscosity the measurements have to be carried out at shear rates of $10^{-3}\,\mathrm{s}^{-1}$ or less, which is very difficult in steady mode, and consequently the dynamic measurements are preferable. The degree of shear thinning can be used for differentiation between linear polymers of narrow and broad molecular weight distribution (more shear thinning). Also, more shear thinning implies a higher degree of long chain branching. Strong temperature dependence of viscosity indicates a branched polyethylene, while a weak dependence indicates a linear polyethylene (the temperature sensitivity factor in the exponential model is about $b = 0.01$ for HDPE and $b = 0.02 - 0.03$ for LDPE).

From the shape of the viscosity curve more information can be inferred relating to other polymer characteristics and properties. Higher shear thinning implies broader molecular weight distribution, which in turn implies more elasticity, and this is turn implies, larger first normal stress difference, larger extrudate swell, and longer stress relaxation. The polymer elasticity is also related to several end-use properties, such as warpage (more) and environmental stress cracking resistance (higher).

1.7.3 Using the Storage Modulus G'

Storage modulus measurement is the most reliable method for determining the elasticity of a polymer melt, which in turn is related to several other processing and end-use properties. Higher G' at low frequencies (higher elasticity) implies a longer high molecular weight tail in the molecular weight distribution curve. During processing, the more elastic polymers tend to develop larger normal stresses which result in larger extrudate swell. Also, upon cooling of the finished product more stresses, are frozen in, which may be released on reheating, and this results in more warpage. The environmental stress cracking resistance is usually higher for the more elastic polymers. Differences between polymers that cannot be detected using the melt flow index and the viscosity curve may show up very clearly in comparing G' data, especially at very low frequencies.

1.7.4 Using Extensional Viscosity

Several processes involve extensional flow, such film blowing, blow molding, thermoforming, and fiber spinning. The polymers to be used in such processing operations should, therefore, be characterized by their extensional properties. LDPE (branched) exhibits high extensional viscosity and strong strain hardening and, consequently, produces stable bubbles in film blowing. LLDPE exhibits lower extensional viscosity than LDPE without any significant strain hardening and produces bubbles that may be prone to instabilities. For such materials the cooling and bubble handling systems downstream of the die lips have to be expertly designed to reduce or eliminate the instabilities. Conventional PP exhibits very low resistance in extension and cannot be processed in conventional film blowing lines. A blown film line for such a material requires extrusion downwards, cooling, reheating and then formation of a bubble. However, newer PP grades with long chain branching can be processed in conventional blown film lines, because the long chain branching provides the required level of extensional viscosity.

In the process of thermoforming the level of extensional viscosity is very important. Very low extensional viscosity materials are not thermoformable. However, when the extensional viscosity is very high, it may be difficult for the sheet to form in the exact shape of corners or other intricate mold geometry.

In foaming of thermoplastics usually low extensional viscosity usually results in bubble collapse and poor bubble structure. Very high extensional viscosity may result in difficulties in the bubble formation process.

1.7.5 Troubleshooting Co-Extrusion

There are two rheological phenomena that manifest themselves during the flow of immiscible polymer melts through dies: layer nonuniformity and interfacial instability [21, 24, 36, 37].

Layer nonuniformity in coextrusion flows is caused mainly by the less viscous polymer going to the high shear region (i.e., the wall) thereby producing encapsulation. Partial encapsulation can occur in common types and sizes of dies, and complete encapsulation is possible for extremely long dies. Differences in polymer wall adhesion and viscoelastic characteristics can also be contributing factors. Weak secondary flows caused by viscoelastic effects (from the second normal stress difference) have been demonstrated to produce layer nonuniformities even when co-extruding differently colored polymer streams of the same polymer [31]. This defect can be reduced by choosing materials with the smallest possible differences in viscosity and viscoelasticity (G', G'', extrudate swell), or by adjusting the stream temperatures to bring the polymer viscosities closer to one another.

Layer nonuniformity can also arise in feedblock co-extrusion, in which melt streams are merged into a single stream in a feedblock before entering the flat die. Uneven flow leakage from the flat die manifold to the downstream die sections can lead to encapsulation of the more viscous polymer by the less viscous, or even the reverse! Feedblock profiling is used to counteract the natural tendency for encapsulation due to viscosity differences [38]. This involves contouring the feedblock flow passages for regions of high or low volumetric throughput, as shown in Figure 1.10. Feedblock profiling combined with eliminating uneven flow leakage from the feeding section of a flat die (or the use of this leakage to counteract the natural tendency for encapsulation) can be used to produce layer-to-layer uniformity in the extrudate. The problem is much more complex when co-extruding many layers, as profiling for one layer will disrupt the other layers. The influence of a feedblock design change is virtually impossible to predict accurately, at present. Powerful computer machinery would be needed to determine the interfaces and interactions with the walls. This is not an exercise for routine equipment design purposes.

Interfacial instability in co-extrusion refers to two common defects consisting of highly irregular or sometimes regular waviness that appears in co-extruded structures at the polymer–polymer interface. The effect is to significantly reduce the optical quality of coextruded film. It is an internal defect, which distinguishes it from sharkskin, which is a surface defect.

The most frequently encountered interfacial instability is zigzag (also known as die-land) instability [36, 37], which appears as chevrons pointing in the flow direction. It is initiated in the die land (which is the parallel wall die section) and is characterized by a critical interfacial shear stress, in the range of 40–80 kPa (roughly a quarter to a half of the critical wall shear stress level for sharkskin). This problem can arise even if adjacent layers are of the same material. The mechanism responsible has not been conclusively identified. Apparently there is amplification of certain disturbance wavelengths under high stress conditions.

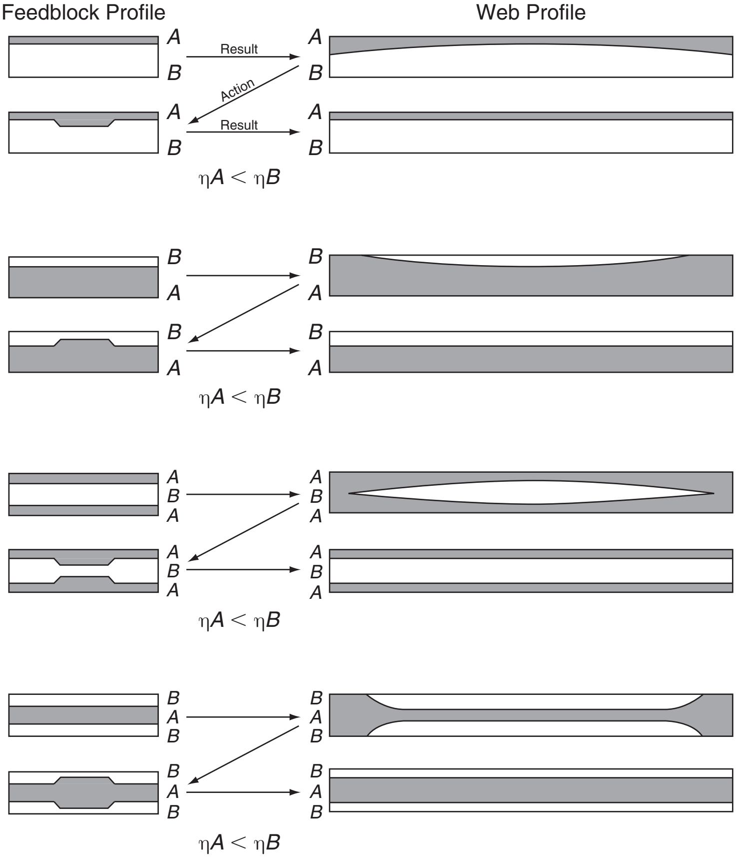

FIGURE 1.10 Feedblock profiling and the resultant effects.

Viscoelasticity is probably a contributing factor, i.e., the interfacial normal stress difference is important. Unfortunately, this is impossible to measure and difficult to calculate accurately. The most reliable means of diagnosing zigzag instability at present is to calculate interfacial shear stress using simulation software. Zigzag instability problems are remedied by reducing interfacial shear stresses.

1.7.6 Using Computer Simulation and Rheological Data

Computer simulation can be very effective in process troubleshooting. First requirement is the existence of reliable viscosity data over a wide range of shear rates, e.g., for extrusion the viscosity must be known from less than $1\,\mathrm{s}^{-1}$ to more than $1000\,\mathrm{s}^{-1}$, while in injection molding the shear rates may reach or exceed $10{,}000\,\mathrm{s}^{-1}$. The second step is for the data to be fitted to a suitable viscosity model such as power law, Carreau–Yasuda, or Cross, with temperature dependence. The third step is to carry out the simulation and perhaps several what-ifs, so possible causes of observed problems can be identified. The simulation data are then compared to whatever observations and measurements are available from the factory floor.

Of course, it all depends on how good the computer software is. If we assume that the software is capable of providing reasonably error-free results, then local pressure, shear rates, shear stresses, temperatures, and streamline patterns are very useful in the troubleshooting process.

Process engineers working on a production line may be biased about a process problem or product defect. Usually, when there are visible extrudate defects they are blamed to sharkskin–melt fracture. However, other problems such as material degradation due to excessive residence time at very high temperatures or die flow lines might be responsible. If the computed die lip shear stress is low ($<0.1\,\text{MPa}$), then sharkskin–melt fracture can be excluded and other causes must be sought. If there is a region of nearly stagnant flow region (low wall shear rates) this might be the source of polymer degradation. In transparent film production, if there are wall shear rates $<5\,\text{s}^{-1}$ anywhere, they are likely to result in degradation related defects, which may appear as black spots, haziness, die lines, or streaks.

Rheological data are of crucial importance, especially when comparing different production batches with differences in the incoming raw material. Again, computer simulations can provide the local pressures, shear rates, shear stresses, and flow patterns, and potential root causes of the problems and defects can be identified.

In special cases, viscoelastic constitutive equations, which can be fitted to reliable rheological data, can be used for simulations. Even if reliable flow simulation is not feasible with a viscoelastic constitutive equation, we can use flow patterns based on GNF and then use the viscoelastic equation to determine post-processing effects, such as shrinkage and warpage. It is also possible for the user to make reasonable approximations and limit a viscoelastic flow analysis to only a region of interest, which might be a die lip exit in extrusion, a sudden restriction in injection molding, or sheet thinning near a corner in thermoforming. Despite the limited predictive ability of the viscoelastic constitutive equations, certain trends might be identified.

1.8 CONCLUDING REMARKS

The rheological characterization of molten polymers is of paramount importance in polymer processing for several reasons. First, viscosity measurements are necessary for equipment design. It is important that the viscosity be measured over the full shear range rate expected in the process. Second, rheological measurements can be used to identify or to differentiate various polymer grades. For such purposes it might be necessary to measure, in addition to the steady shear viscosity, the extensional viscosity and the storage and loss moduli.

Occasionally, measurements of normal stress differences might provide significant insight into the materials or the processes.

Rheological measurements are usually more sensitive and easier than other methods of characterization, and they are excellent tools for process troubleshooting and optimization purposes. The viscoelastic models provide significant insight into polymer behavior, but they are not used in routine equipment design, due to mathematical complexities and limited predictive power for industrial operating conditions.

REFERENCES

1. R.B. Bird, R.C. Armstrong, and O. Hassager, *Dynamics of Polymeric Liquids*, vol. 1, Wiley, New York, 1987.
2. C.W. Macosko, *Rheology: Principles, Measurements and Applications*, VCH Publishers, New York, 1994.
3. F.N. Cogswell, *Polymer Melt Rheology*, Woodhead Publishing, Cambridge, UK, 1996.
4. A.V. Chenoy and D.R. Saini, *Thermoplastic Melt Rheology and Processing*, Marcel Dekker, New York, 1996.
5. J.M. Dealy and K.F. Wissbrun, *Melt Rheology and Its Role in Plastics Processing*, Chapman & Hall, London, 1996.
6. R.I. Tanner, *Engineering Rheology*, Oxford Engineering Science, Oxford, UK, 2000.
7. C.D. Han, *Rheology and Processing of Polymeric Material*, vols. 1–2, Oxford University Press, Oxford, UK, 2007.
8. A.Y. Malkin and A.I. Isayev, *Rheology*, ChemTech Publishing, Toronto, 2006.
9. W.W. Graessley, *Polymeric Liquids and Networks: Dynamics and Rheology*, Garland Science, London, 2008.
10. J.L. White, *Principles of Polymer Engineering Rheology*, Wiley, New York, 1990.
11. M.T. Shaw and W.J. MacKnight, *Introduction to Polymer Viscoelasticity*, Wiley, New York, 2005.
12. J.M. Dealy and R.G. Larson, *Structure and Rheology of Molten Polymers*, Hanser, Munich, 2006.
13. R.K. Gupta, *Polymer and Composite Rheology*, Marcel Dekker, New York, 2000.
14. J.L. Leblanc, *Filled Polymers*, CRC Press, Boca Raton, 2010.
15. J. Vlachopoulos and J.R. Wagner, eds., *The SPE Guide on Extrusion Technology and Troubleshooting*, Society of Plastics Engineers, Brookfield, CT, 2001.
16. S. Middleman, *Fundamentals of Polymer Processing*, McGraw-Hill, New York, 1977.
17. Z. Tadmor and C.G. Gogos, *Principles of Polymer Processing*, Wiley, New York, 2006.
18. R.G. Griskey, *Polymer Process Engineering*, Chapman & Hall, New York, 1995.
19. M.M. Denn, *Polymer Melt Processing*, Cambridge University Press, Cambridge, UK, 2008.

20. T. Kanai and G.A. Campbell, eds., *Film Processing*, Hanser, Munich, 1999.
21. J.R. Wagner, ed., *Multilayer Flexible Packaging*, Elsevier, Amsterdam, 2010.
22. D.G. Baird and D.J. Collias, *Polymer Processing Principles and Design*, Wiley, New York, 1998.
23. C.I. Chung, *Extrusion of Polymers*, Hanser, Munich, 2000.
24. T.J. Butler, ed., *Film Extrusion Manual*, TAPPI Press, Atlanta, GA, 2005.
25. M. Kamal, A. Isayef, and S. Liu, *Injection Molding Fundamentals and Applications*, Hanser, Munich, 2009.
26. M.M. Denn, *Ann. Rev. Fluid Mech.*, 33, 265 (2001).
27. S.G. Hatzikiriakos and K. Migler, eds., *Polymer Processing Instabilities: Control and Understanding*, Marcel Dekker, New York, 2004.
28. M. Sentmanat, B.N. Wang, and G.H. McKinley, *J. Rheol.*, 49, 585 (2005).
29. J. Vlachopoulos, *Rev. Def. Beh. Mat.*, 3, 219 (1981).
30. B. Debbaut, T. Avalosse, J. Dooley, and K. Hughes, *J. Non-Newt. Fluid Mech.,* 69, 255 (1997).
31. J. Dooley, "*Viscoelastic Flow Effects in Multilayer Polymer Coextrusion,*" doctoral thesis, University of Eindhoven, Netherlands, 2002.
32. S.W. Shang, *Adv. Polym. Tech.*, 12, 389 (1993).
33. H.M. Laun, *J. Rheol.*, 30, 459 (1986).
34. E. Mitsoulis, *J. Non-Newt. Fluid M.*, 97, 13 (2001).
35. T.C.B. McLeish and R.G Larson, *J. Rheol.*, 42, 81 (1998).
36. R. Shroff and H. Mavridis, *Plast. Techn.*, 37, #2, 5 (1998).
37. J. Perdikoulias and C. Tzoganakis, *Plast. Eng.*, 52, #4, 41 (1996).
38. P. Cloeren, in *Proceedings of S.P.E. Extrusion Division RETEC*, Toronto, Canada, 1993.